Landmarks in Earth Reinforcement, Ochiai et al. (eds),
© 2001 Swets & Zeitlinger, ISBN 90 2651 863 3

Modelling of reinforced unpaved composite material using HISS model

K.G. Sharma & K.K. Gupta
Department of Civil Engineering, IIT Delhi, India
Praveen Aggarwal
Department of Civil Engineering, REC Kurukshetra, India

ABSTRACT: With the advent of high strength geogrids, the interest of civil engineers in using geosynthetics as reinforcement material in pavement construction has increased. An experimental study is carried out at IIT Delhi to understand the effect of geogrid in unpaved roads. Behavior of composite material, which comprises of Yamuna sand as subgrade and Water Bound Macadam (WBM) as base course is studied with and without geogrid reinforcement under drained conditions. The geogrid manufactured by Netlon India product code CE201 is used as reinforcing material. Drained triaxial tests were performed at three different confining pressures of 50, 100 and 200 kPa on both unreinforced composite and reinforced composite materials of specimen size 100mm diameter and 200mm height. Hierarchical single surface (HISS) model developed by Desai and coworkers is used to model the unreinforced and reinforced composite material. A computer program PARA6 is used to calculate the various parameters and to back predict the stress-strain-volume change behavior of unreinforced and reinforced composite materials. The predicted results match closely with the observed results.

1 INTRODUCTION

Pavement is a structure made in between the wheel and the natural ground. The basic aim of pavement is to provide a hard surface for the movement of wheels without significant deformation and to distribute the wheel load effectively to the larger area of natural ground so that the stresses are within bearing capaity. Temporary or unpaved roads with low volume of traffic are required for construction and access roads, contractors' haul roads, short-term detour around, for example, bridge replacement construction etc. Further such roads are also frequently constructed world wide to support resource industry viz. forestry, mining, oil and tarsand extraction, agriculture and others.

Considering the economic significance of unpaved road, attempts have been made to understand their behavior, so that the benefit of geosynthetic can be quantified. Initially low strength geotextiles were used as a separation layer only thereby maintaining the effective thickness. Reinforcement function of geosynthetics was realized with the emergence of improved material in the form of strong woven geotextile and geogrids. Various factors, which affect the behavior of soils, are density of the soil, the confining pressure, the drainage conditions and the stress path followed. Stress-strain relationships of the soils are important to be studied to analyze load-deformation problems. Reinforced soils have further complex behavior due to insertion of the reinforcement. The behavior is dependent on many additional factors such as the quantity, type, spacing, interface properties and tensile strength of the reinforcement. Stress-strain relationship of reinforced soil is thus function of these factors in addition to the other factors of unreinforced soil.

A number of experimental and analytical studies have been undertaken by researchers to understand the behavior of the reinforced soils. For interface friction behavior, modified direct shear test or pullout test has been used. Stress-strain and strength characteristics have been studied mostly by conducting triaxial tests.

Triaxial tests were conducted on cylindrical specimen of reinforced sand using woven fabric glass netting as reinforcement (Yang 1972). It was observed that the axial stress increased with the number of reinforcement layers. Axial strain at failure also inereased due to insertion of the reinforcement. Strength of the reinforced soil was observed to be increasing with the number of reinforcement layers.

Constitutive model is a mathematical relation, which reproduces the observed response of a continuous medium. Constitutive models can be broadly classified into following three categories.

1. Empirical models
2. Elasto- plastic models
3. Elasto-viscoplastic models

All geological materials show plasticity almost from the beginning. Therefore, stress-strain and volume change response of many geologic media includ-

ing water bound macadam, bituminous conerete can only be predicted by plasticity models. Some of the yield criteria are

1. Mohr-Coulomb Criterion
2. Drucker-Prager Yield Criterion
3. Critical State Model
4. HISS model

Two models, the SIGMA-model and TAU-model were postulated using Yang's results for describing the strength of soil mass reinforced with horizontal layers (Hausmann 1976). Broms (1977) suggested a semi-empirical formula to evaluate the strength of reinforced soil in a triaxial test. He further observed that placement of reinforcement plays an important role in the behavior of reinforced soils. The empirical relation was however very complex. Rao et al. (1987) attempted to model the results with hyperbolic model. All these studies were conducted using conventional triaxial compression stress path. Baykal et al. (1992) conducted triaxial tests using two stress paths and observed that stress-strain behavior of reinforced soil is stress path dependent. Soni (1995) studied the behavior of reinforced soil using six stress paths and modelled the behavior using HISS model.

2 ROLE OF GEOSYNTHETICS IN UNPAVED ROADS

The use of geosynthetics in the pavement construction started to serve as a separation layer. An example of use of geosynthetics as separation layer is in the construction of airfield in Switzerland (Hausman 1987). With the development of new stronger geosynthetics reinforcement funetion of this new construction material became apparent. Today geosynthetics are used in the pavement construction primarily to serve the following four functions:

1. Separation
2. Filtration
3. Drainage
4. Reinforcement

2.1 *Behavior of reinforced flexible pavement*

The strengthening effect of geosynthetics in flexible pavement has been studied through plate bearing tests on laboratory models and through triaxial tests under static and repeated loading.

Barenberg et al. (1975), Binquet & Lee (1975) stressed on the mode of failure and the bearing capacity of the systems. According to Barenberg et al. (1975) non-woven geotextile inhibits the punching type failure characteristics of soft soil by restraining the soft subgrade and they proposed to use higher bearing capacity factors in reinforced system irrespective of the mechanical properties of geotextiles. Similar observation was made by Steward et al. (1977) in a test road with non-woven geotextile.

Later on Webster & Watkins (1977), Kinney (1979) indicated that the performance of such systems improved with modulus of geotextile and led to the inclusion of membrane effect in theoretical analysis and design procedures proposed by Barenberg (1980). Giroud & Noriray (1981). Raumann (1982). Haliburton & Barron (1983) proposed the restraint action of geotextiles on the aggregate layer.

Limited stu dies have been done on reinforced pavement system under repeated loading. From the above literature it is very clear that a geotextile effectively reduces the permanent deformation of the reinforced pavement system. The beneficial effect of the geotextile in controlling the evolution of permanent deformation appears to be due to the following reasons (Barksdala et al. 1982 & Kinney 1982).

1. Geotextile at the interface improves the load spreading capacity of the aggregate consequently the stress-strain state in the subgrade changes leading to less plastic strain with number of repetitions.

2. Lateral restraint effect of geotextile restricts the lateral movement of the subgrade soil away from the directly loaded zone.

Kinney (1982) observed that as the thickness of the aggregate increases the beneficial effect decreases and also some lateral extensions beyond the directly loaded area is essential for better performance. On the other hand, Dougles & Kelly (1986) found that anchorage details of geotextile do not effect the behavior of unpaved models.

Omoto et al. (1992) observed the cumulative permanent and elastic deformations at the surface under repetitive load tests on aggregate-soil system with and without reinforcement at the interface. From the results it is concluded that under similar test conditions geosynthetics can reduce the elastic deformation on such systems thereby improving the resilient modulus of the system.

3 HISS MODEL

In the present study HISS model is used. The brief description of the model is as follows. Desai (1980), Desai et al. (1986) developed hierarchical single surface (HISS) δ_0 and δ_1 models. In these models, a unique and continuous yield function is used that leads to the failure when an ultimate condition is reached. The δ_0 model is based on associative plasticity and isotropic hardening.

The constitutive equation for elasto-plasticity can be written as

$$d\sigma_{ij} = C^{EP}_{ijkl} d\varepsilon_{kl} \quad (1)$$

where C^{EP}_{ijkl} is the constitutive matrix for elastoplastic approach.

The yield function for δ_0 model is given as

$$F = \left(\frac{J_{2D}}{P_a^2}\right) - \left[-\alpha\left(\frac{J_1}{P_a}\right)^n + \gamma\left(\frac{J_1}{P_a}\right)^2\right](1-\beta S_r)^m \quad (2)$$

$$S_r = \text{Stress ratio} = \frac{\sqrt{27}}{2}\frac{J_{3D}}{J_{2D}^{1.5}} \quad (3)$$

where:

J_1 first invariant of stress tensor
J_{2D} second invariant of deviatoric stress tensor
J_{3D} third invariant of deviatoric stress tensor
P_a atmospheric pressure
α, β, n and γ material constants
m -0.5 for geological materials (Desai et al. 1986).

For non-associative model δ_1, plastic potential function Q is defined as a modification of F with α replaced by α_Q, i.e.,

$$Q = \left(\frac{J_{2D}}{P_a^2}\right) - \left[-\alpha_Q\left(\frac{J_1}{P_a}\right)^n + \gamma\left(\frac{J_1}{P_a}\right)^2\right](1-\beta S_r)^m \quad (4)$$

where:

$$\alpha_Q = \alpha + \kappa(\alpha_0 - \alpha)(1 - r_v) \quad (5)$$

in which κ is non-associative parameter, α_0 is α at the beginning of shear loading and $r_v = \frac{\xi_v}{\xi}$, ξ_v is volumetric part of ξ (plastic strain trajectory).

3.1 *Properties of the HISS yield function*

Some of the features of HISS model are as follows:

1. The model involves only one continous surface which describe yield or loading surfaces by a single function and also describe the ultimate behaviour. In the model only two parameters γ and β at ultimate are used to define the traditional failure.
2. Entire hardening and ultimate behaviour is defined by only one function.
3. The plot of yield function F is continous and convex in the stress space for geological material. However it intersects the J_1 axis at right angles, as a result it can be implemented in the context of the classical theory of plasticity.
4. As the intersection of two or more surfaces and corner in Π plane are avoided, the model is easier to implement in numerical analysis.
5. A single parameter growth function α can simulate hardening and include the effect of stress path, volume change and coupling of shear and volumetric responses.

4 DETERMINATION OF MATERIAL CONSTANTS

The HISS model requires ni ne parameters for the constitutive modelling of any material, which can be classified into five categories.

1. Elastic constants (E, v)
2. Ultimate parameters (γ, β, m).
3. Phase change parameter (n).
4. Hardening parameters a_1, η_1.
5. Non-associative parameter (κ).

The procedure for the determination of material parameters has been described in detail in various references (Varadarajan & Desai 1993, Desai 1994). It is briefly presented herein.

1. Elastic constants (E, v)

The two elastic constants for an isotropic material. Young's modulus, E and Poisson's Ratio, v are determined from the average slopes of the initial part of the stress-strain curves and the ratio of lateral and axial strains respectively. Janbu's relation is used to correlate Young's modulus with confining pressure.

$$E = kP_a\left[\frac{\sigma_3}{P_a}\right]^N \quad (6)$$

where k and N are constants.

2. Ultimate parameters (γ, β, m)

For many geological materials m is found to be -0.5 (Desai et al. 1986). Therefore. in the present work, m is considered as -0.5. The procedure adopted for the calculation of γ and β from the laboratory results is described below.

At the ultimate state, the value of α tends to zero thus, the yield surface degenerates to an open surface intersecting J_1 axis at infinity. Applying the condition to the yield function, Equation 1, the slope of the ultimate line is derived as

$$\frac{J_1}{\sqrt{J_{2D}}} = \left[\frac{(1-\beta S_r)^{1/2}}{\gamma}\right]^{1/2} \quad (7)$$

where: $S_r = 1$ for compression path and $S_r = -1$ for extension path. The ultimate parameters can be found out by conducting least square fitting procedure on Equation 7 for at least two triaxial tests on $J_1 - \sqrt{J_{2D}}$ plane.

3. Phase change parameter (n)

The phase change parameter, n, is calculated using the zero plastic volume change condition, $\frac{\partial F}{\partial J_1} = 0$. An average of n values for different tests is taken as an overall value of n for the material.

4. Hardening parameters (a_1 and η_1)

In the present study, growth function α is assumed as the function of ξ as

$$\alpha = \frac{a_1}{\xi^{\eta_1}} \quad (8)$$

Taking natural log on both sides of Equation 8 gives,

$$\ln(\alpha) = \ln(a_1) - \eta_1 \ln(\xi) \quad (9)$$

a_1 and η_1 are determined from the least square fitting procedure for each test. The average value of a_1 and

η_1 from various tests are taken as overall values of the hardening parameters.

5. Non-associative parameter (κ)

Non-associative parameter, κ in the plastic potential formation, Q is assumed as constant and is determined from the conditions near the ultimate. Basic steps in evaluating, κ are given below.

From the flow rule,

$$d\varepsilon_{ij}^p = \lambda \frac{\partial Q}{\partial \sigma_{ij}} \tag{10}$$

we get

$$d\varepsilon_v^p = \lambda \left[\frac{\partial Q}{\partial J_1} \frac{\partial J_1}{\partial \sigma_{11}} + \frac{\partial Q}{\partial J_1} \cdot \frac{\partial J_1}{\partial \sigma_{22}} + \frac{\partial Q}{\partial J_1} \cdot \frac{\partial J_1}{\partial \sigma_{33}} \right] \tag{11}$$

or

$$d\varepsilon_v^p = 3\lambda \frac{\partial Q}{\partial J_1} \tag{12}$$

$$\left(\frac{d\varepsilon_v^p}{d\varepsilon_{11}^p} \right) = \frac{(3\frac{\partial Q}{\partial J_1})}{(\frac{\partial Q}{\partial \sigma_{11}})} = \upsilon^p \tag{13}$$

Then from Equation 5,

$$\kappa = (\alpha_0 - \alpha) / \left[(\alpha_0 - \alpha)(1 - r_\upsilon) \right]$$

Even though, κ could be calculated for any stress point, t he portion of $\varepsilon_\upsilon - \varepsilon_1$, curve near the ultimate coudition is used since the deviation $(\alpha_Q - \alpha)$ is the greatest in the ultimate zone. The value of κ has been calculated using the program PARA6.

5 TEST PROGRAM

In order to model the unreinforced and reinforced unpaved composite materials, a series of drained triaxial test is carried out on unreinforced and reinforced unpaved composite materials at three contining pressures of 50, 100 and 200 kPa.

5.1 *Materials*

Subgrade Soil

The subgrade soil used in the present study is Yamuna Sand. Yamuna Sand is locally available sand obtained from the bed of river Yamuna. The characteristics of Yamuna sand are summarized in Table 1.

Aggregates

Two grades of crushed stone aggregates were used to prepare the Water Bound Macadam (WBM) mix. The particle size distribution of the two grades of aggregates is shown in Figure 1. The grade A is used as coarse aggregates and grade B as screening.

The two grades of crushed stone aggregates A and B were mixed with binder having grade C (P.I. = 6), in the ratio of 1.0 : 0.16 : 0.15 by volume in loose state to obtain the required gradation for the WBM mix (IRC: 19-1977).

Table 1. Characteristics of Yamuna Sand.

Property	Value
% Sand	94
% Silt	6
Specific Gravity (SG)	2.67
Coefficient of Uniformity C_u	2.24
Coefficient of Curvature C_s	1. 14
Maximum Dry Density ($\gamma_{d\ max.}$)	16 kN/m^2
Minimum Dry Density ($\gamma_{d\ min.}$)	13 kN/m^2

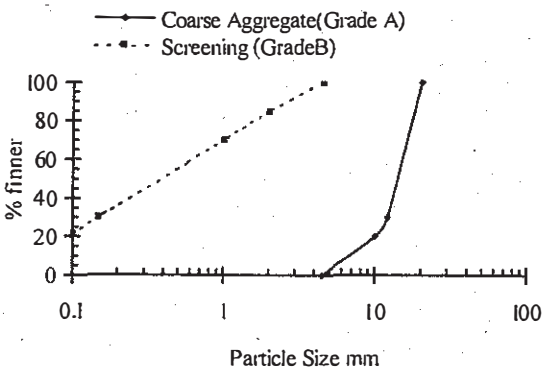

Figure 1. Gradation of Water Bound Macadam.

Water Bound Macadam (WBM) mix design

Water Bound Macadam mix was designed as per (IRC: 19-1977) specification, for possible use as surfacing course. Delhi Silt (P.I = 6%) was used as a binding material. Required quantity of both the grades A and B (Coarse aggregate and Screening) was mixed with binding material in the ratio of 1.0 : 0.16 : 0.15 by volume in loose state in dry condition. Then Proctor Compaction Test was carried out to find out the Optimum Moisture Content (OMC) and Maximum Dry Density (MDD) for further use. OMC for WBM is 6.8 % and MDD achieved at this moisture content is 22.30 kN/m^3.

Geogrid

The geogrid used was extruded mesh CE 201, manufactured by M/s Netlon India Ltd., Vadodara. Aperture size is 7.1 × 7.1 mm. thickness 1.85 mm and at joint is 3.25 mm. The wide width tension tests were carried out as per (ASTM:D-4595-86 1988) to determine the load deformation behavior in machine and cross directions of geogrid. Tensile strength is 7.11 and 6.43 kN/m in machine and cross directions respectively at 40 mm elongation.

5.2 *Testing*

Triaxial test

Conventional triaxial apparatus (Bishop & Henkel 1962) was used for the triaxial tests. A perspex triaxial cell capable of withstanding more than 1 MPa

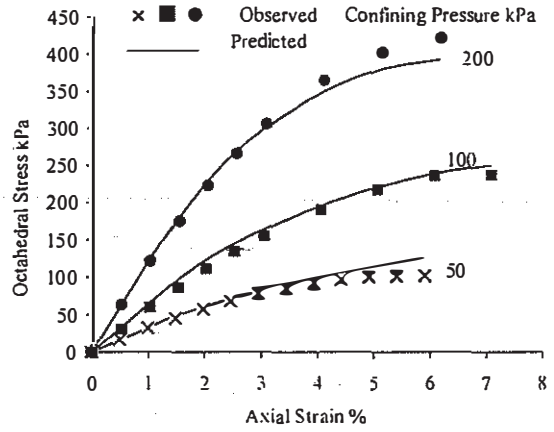

Figure 2. Variation of octahedral stress with arial strain for unreinforced composite material.

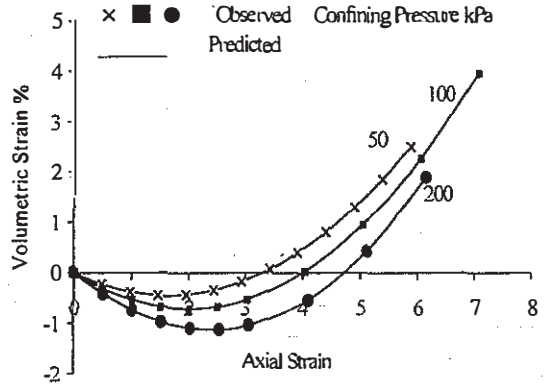

Figure 3. Variation of volumetric strain with axial strain for unreinforced composite material.

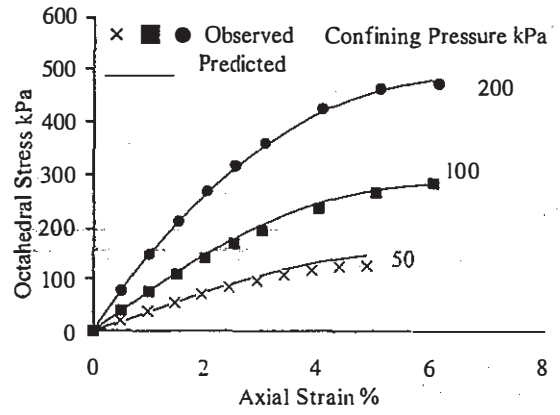

Figure 4. Variation of octahedral stress with axial strain for reinforced composite material.

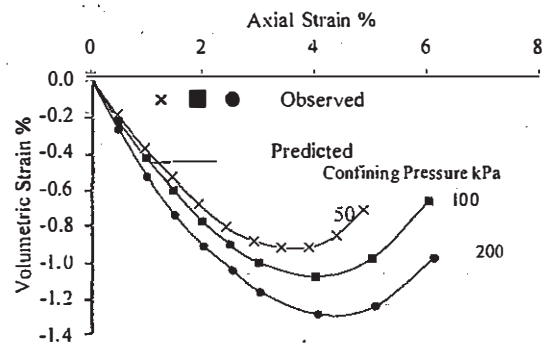

Figure 5. Variation of volumetric strain with axial strain for reinforced composite material.

and with the facility of 100 mm diameter and 200 mm height was used. Thickness of subgrade (Yamuna sand) and base course layer (WBM) is 100mm each in both the cases. Axial strains, deviator stresses and volumetric strains were observed during the tests. It is observed that mode of failure of unreinforced composite material is by bulging of the subgrade layer, hence reinforcement is provided at the center of the subgrade layer in reinforced composite material specimen. The experimentally observed behavior is presented in Figures 2–5.

6 MODELLING

All the nine constants for HISS model are calculated for both unreinforced and reinforced cases and are presented in Table 2.

7 PREDICTION

The incremental constitutive relation (Equation 1) has been used to predict the stress-strain-volume change response. The equation is integrated starting from the initial hydrostatic state. The prediction is made using the nine parameters calculated for unreinforced and reinforced composite material under strain control condition. Both predicted and experimentally observed variation of octahedral stress and volumetric strain with axial strain are presented in Figures 2–3 for unreinforced case and in Figures 4–5 for reinforced case. The observed and predicted behavior matches closely.

Table 2. The material parameters for unreinforced and reinforced composite materials.

Constant	Unreinforced	Reinforced
k	141.97	171.58
N	1.1280	1.0996
γ	0.0798	0.0840
β	0.74	0.74
m	−0.5	−0.5
n	2.655	2.820
a_1	0.001150	0.000215
η_1	0.420	0.686
κ	0.15	0.22

8 CONCLUSIONS

From the results it is observed that inclusion of geogrid improves the performance of composite material by more than 15%. Dilation starts at a higher axial strain in case of reinforced composite material as compared to unreinforced composite material. Modelled behavior matches closely with the observed results.

REFERENCES

ASTM: D4595-86 1988. Test method for tensile properties of geotextiles by wide width strip method. ASTM standard of geotextiles. 63-66.ASTM, Philadelphia, PA, USA.

Barenberg, E. J. 1980. Design procedures for soil-fabric aggregate systems with mirafi 500x fabrics University of Illinois at Urbana: Champaign.

Barenberg, E. J., Dowland, J. H. Jr. & Hales, J.II 1975. Evaluation of soil-aggregate systems with mirafi fabric. Department of Civil Engineering. University of Illinois.

Barksdale, R., Robnett, Q., Lai, J. & Zeevaert-Wolff, A. 1982. Experimental and theoretical behavior of geotextile reinforced aggregate soil systems. *Proc. 2nd. Int. Conf on Geotextiles,* Las Vegas, Vol. 2, 375–380, USA.

Baykal, G., Guler, E. & Akkol, O. 1992. Comparison of woven and non-woven geotextile reinforcement using stress path tests. *Proc. Int. sym. on Earth Reinforcement,* Kyushu, 23–27, Japan.

Binquet , J. & Lee, K. L. 1975. Bearing capacity tests on reinforced earth slabs. *Proc. ASCE Jn. of Geotechnical Engineering Div.,* Vol. 101, No. GT 12, 1241–1255.

Bishop, A. W. & Henkel, D. J. 1962. The measurement of soil properties in the triaxial test. Edward Arnold Publishers ltd., London.

Broms, B. B. 1977. Triaxial tests with fabric reinforced soil. *Proc. Int. Conf. on the use of fabric in geotechnics,* Paris, 129–133.

Desai, C. S. 1980. A general basis for yield, failure and potential functions in plasticity. *Int. Journ. Num. Anal. Meth. Ceomech.,* 15(9), 649–680.

Desai, C. S., Somasundaram, S. & Frantziskonis, G. 1986. A hierarchical approach for constitutive modelling of geologic materials. *Int. J. Num. and Analytical Methods in Geomech.,* 10, 225–257.

Desai, C. S. 1994. Hierarchical single surface and the disturbed state constitutive models with emphasis on geotechnical applications. Geotech. Eng. Emerging Trends in Design and Practice, Chap. 5, K. R. Saxena (Editor), New Delhi, India. Oxford & IBH Pub. Co. P t. Ltd.

Douglas, R. A. & Kelly, M. A. 1986. Geotextile reinforced unpaved logging roads: the effect of anchorage. *Geotextiles and Geomembranes,* Vol. 4, 93–106.

Giroud, J. P. & Noiray, L. 1981. Geotextile reinforced unpaved road design. *Proc. ASCE Jn. Geotechnical Engineering Div.* Vol. 107, No. GT9, 1233–1254.

Haliburton, T. A. & Barron, J. V. 1983. Optimum depth method for design of fabric reinforced unsurfaced roads. Presented at the Annual Meeting, Transportation Research Record Board.

Hausmann, M. R. 1987. Geotextiles for unpaved roads – A review of design procedures. *Geolextiles and Geomembranes,* Vol. 5, 201–223.

Hausmann, M. R. 1976. Strength of reinforced soil. *Proc. 8th Australian Road Board Conf.,* 8(13): 1–8.

IRC: 19-1977 1982. Standard specification and code of practice for water bound macadam. *The Indian Road Congress,* New Delhi, India.

Kinney, T. S. 1979. Fabric induced changes in high defonnation soil-fabric-aggregate systems. Ph.D. Thesis. Graduate College. University of Illinois, Urbana, USA.

Kinney, T. C. 1982. Small scale load test on a soil-geotextileaggregate system. *Proc. 2nd Int. Conf. on Geotextiles,* Vol. 2, 405–409, Las Vegas, USA.

Omoto, S., Kawabata, K. & Mizobuchi, M. 199?. Reinforcement effect of geotextiles on pavement with weak subgrade. Earth Reinforcement Practice: 671-676. Eds. Ochiai, Hayashi and Otani. Rotterdam: Balkema.

Rao, G. V., Gupta, K. K. & Kachhawah, R. 1987. Triaxial behavior of geotextile reinforced sand. *Proc. Indian Geot. Conf.* Bangalore, 1: 323–328, India.

Raumann, G. 1982. Geotextiles in unpaved roads: desi~n considerations. *Proc. 2nd Int. Conf. on Geotextiles,* Vol. 2. 417–422. Las Vegas, USA.

Soni, K. M. 1995. Constitutive modelling of reinforced soil. Ph.D. Thesis, Indian Institute of Technology, Delhi, India.

Steward, J., Williamson, R. & Moheny, J. 1977. Guidelines for use of fabric in construction of low-volume roads. USDA. Forest Service, Portland. Oregon.

Varadarajan, A. & Desai, C. S. 1993. Material constants of a constitutive model determination and use. *Indian Geotech. J.,* 23(3), 291–313.

Webester, S. L. & Watkins, E. J. 1977. Investigation of construction techniques for tactical bridge approach roads across soft ground. Technical Report 5-77-1, US Army Engineers, Waterways Experiment Station, Vicksburg, Miss.

Yang, Z. 1972. Strength and deformation characteristics of reinforced sand. Ph.D thesis, University of California, Los Angeles, USA.